Black Phosphorus (BP) Nanodots for Potential Biomedical Applications

Hyun Uk Lee, So Young Park, Soon Chang Lee, Saehae Choi, Soonjoo Seo, Hyeran Kim, Jonghan Won, Kyuseok Choi, Kyoung Suk Kang, Hyun Gyu Park, Hee-Sik Kim, Ha Rim An, Kwang-Hun Jeong, Young-Chul Lee, and Jouhahn Lee**

Recently, the appeal of 2D black phosphorus (BP) has been rising due to its unique optical and electronic properties with a tunable band gap (≈0.3–1.5 eV). While numerous research efforts have recently been devoted to nano- and optoelectronic applications of BP, no attention has been paid to promising medical applications. In this article, the preparation of BP-nanodots of a few nm to <20 nm with an average diameter of ≈10 nm and height of ≈8.7 nm is reported by a modified ultrasonication-assisted solution method. Stable formation of nontoxic phosphates and phosphonates from BP crystals with exposure in water or air is observed. As for the BP-nanodot crystals' stability (ionization and persistence of fluorescent intensity) in aqueous solution, after 10 d, ≈80% at 1.5 mg mL^{-1} are degraded (i.e., ionized) in phosphate buffered saline. They showed no or little cytotoxic cell-viability effects in vitro involving blue- and green-fluorescence cell imaging. Thus, BP-nanodots can be considered a promising agent for drug delivery or cellular tracking systems.

1. Introduction

Extremely low-dimensional materials, especially 2D and several-layered materials (graphene, silicene, germanene, and stanene)[1] have been explored for a variety of extraordinary applications such as nanoelectronics,[2–5] energy-storage devices,[6,7] composite materials, and (gas) sensors.[8] However, due to limitations such as the gapless band gap (i.e., the semimetal graphene) and the large and indirect band gap of transition-metal dichalcogenides (TMDCs) including MoS[2] and WSe,[2,9] alternative 2D materials have been persistently researched both theoretically and experimentally. Perhaps most interestingly, atomically thin and 2D black phosphorus (BP) with a direct and tunable

Dr. H. U. Lee, S. Y. Park, Dr. S. Seo, H. Kim, Dr. J. Won, H. R. An, J. Lee
Advanced Nano-Surface Research Group
Korea Basic Science Institute (KBSI)
Daejeon 305-333, South Korea
E-mail: jouhahn@kbsi.re.kr
S. C. Lee
Department of Applied Chemistry and Biological Engineering
Chungnam National University
Daejeon 305-764, South Korea
Dr. S. Choi, Dr. H.-S. Kim
Sustainable Bioresource Research Center
Korea Research Institute of Bioscience & Biotechnology (KRIBB)
Daejeon 305-806, South Korea
DOI: 10.1002/smll.201502756
Dr. K. Choi
Center for Research Facilities
Kunsan National University
Gunsan 573-701, South Korea
K. S. Kang, Prof. H. G. Park
Department of Chemical and Biomolecular Engineering
Korea Advanced Institute of Science and Technology (KAIST)
291 Daehakno, Yuseong-gu, Daejeon 305-701, South Korea
K.-H. Jeong, Y.-C. Lee
Department of BioNano Technology
Gachon University
1342, Seongnamdaero, Sujeong-gu, Seongnam-si
Gyeonggi-do 461-701, South Korea
E-mail: dreamdbs@gachon.ac.kr

band gap, based on the bridging of graphene and TMDCs, are expected to be promising medical-application candidates.[10] In field-effect transistor (FET) devices, BP has demonstrated a higher hole mobility and on/off ratio[11] with reduced current fluctuation.[12] Despite such positive characteristics of 2D BP materials, BP can be easily degraded under exposure to water and air,[13–15] resulting in fast fluorescence decay by photobleaching. Thus far, certain practical (opto)electronic applications of BP crystals, including atomic-layer deposition of Al_2O_3,[12,16] encapsulation in a host molecule,[17] and substitution of Ti metal with P atoms by our group,[18] have been shown to successfully overcome the phosphorus-crystal instability problem under ambient conditions. BP has also attracted great interest in many fields such as composites and sensors,[8] beyond-BP transistors, photodetectors,[19] thin-film solar cells,[20] anode materials in lithium-ion batteries,[6,21,22] as well as applications with previous successes in the utilization of graphene (analogues or derivatives).[23–25]

Very recently, phosphorus has emerged as a biomedical probe that allows drug delivery, bioimaging and further therapeutics. Compared with conventional semiconductor quantum dots associated with long-term toxicity and environmental concerns owing to the use of heavy metals, BP, particularly BP-nanodots, can reduce ecological concerns and economic problems. BP-nanodots are stable in human body systems, permitting their use in biomedical applications because the abundant sources of phosphorus in the environment and its stability, i.e., ionization and persistent of fluorescent intensity in the human body with regards to the release of P_xO_y (usually phosphates and phosphonates) with nontoxic intermediates , which enable higher biocompatibility and health safety.[10,26] Thus, BP-nanodots are becoming a desirable alternative to metal-based quandum dots due to their low cytotoxicity and excellent biocompatibility. In order to achieve BP-based medical agents, it is necessary to demonstrate in vitro mammalian cell toxicity trials for BP and ionized BP treatments, respectively, along with simultaneous investigations of BP-crystal uptake in cells by photoluminescence (PL) bioimaging.

In this article, we report the first study on BP-nanodots for potential biomedical applications. It is focused on high-yield several-layered BP-nanodots, ranging in diameter from a few nm to <20 nm with an average of ≈10 nm, obtained by exfoliation with a modified ultrasonication-assisted solution method. We determined the BP-nanodot degradation lifetime as ionized in aqueous phosphate buffered saline (PBS) buffer solution (≈80% of BP-nanodot crystals at 1.5 mg mL^{-1} were degraded after 10 d). The BP-nanodot crystals' cell viabilities showed little or no cytotoxic effects in vitro and blue and green emissions of BP-nanodots were observed in HeLa cells. These results suggest that our prepared BP-nanodots can be a biological fluorescence agent in medical applications, after in vivo cytotoxicity assays.

2. Results and Discussion

For morphological structures and spectral analysis of BP-nanodots, as shown in **Figure 1**a, each BP-nanodot ranges in diameter from a few nm to <20 nm, with an average width of 10 nm and height of approxmiately 8.7 nm, equivalent to several layers of BP. The X-ray diffraction (XRD) pattern of the BP-nanodots, revealing reflective patterned peaks of d_{020} = 5.2 Å, d_{040} = 2.6 Å, and d_{060} = 1.7 Å at 2θ = 16.9°, 34.2°, and 52.3°, respectively, indicate crystalline BP with orthorhombic structure (Figure 1b) [JCPDS no. 76-1957]. With transmission electron microscopy (TEM), the morphology of the several-layered BP-nanodots, as prepared by the modified ultrasonication-assisted solution method,[17,27] was shown to be well defined, of ≈8 nm and with crystal lattice fringes (Supporting Information, Figure S1).

In optical studies of BP-nanodots, it is indicated the optical properties of the UV–vis absorbance spectrum of the BP-nanodots at 1.0, 0.5, and 0.25 mg mL^{-1} (Supporting Information, Figure S2), revealing a broad absorbance pattern at 200–700 nm wavelengths within a distinctive UV range with an inset digital camera photograph of a vial containing BP-nanodots at 1.0 mg mL^{-1} with a yellow-brown color. In the Raman spectrum and mapped images of the BP-nanodots (**Figure 2**), A1g at 365 cm^{-1}, B2g and A2g were assigned as in-plane modes at 442 and 465 cm^{-1}, respectively; these values, relative to those of BP quantum dots (BPQDs),[26] were blue-shifted ≈2.4, ≈3.3, and 1.1 cm^{-1} at A1g, B2g, and A2g, respectively.

PL spectra were recorded at 290, 310, 330, 350, 370, 390, 410, 430, and 450 nm excitation wavelengths (**Figure 3**a), plotting strong emission peaks at 394, 421, 448, 466, 492, and 516 nm, with a maximum quantum yield of ≈7.2% by summation area, ranging from 400 to 700 nm. After 7 d, the fluorescence intensity was reduced to at least half of the initial level by degradation of BP-nanodots in aqueous solution (Figure 3b). After 10 d, it was confirmed that the stability of the BP-nanodots in PBS buffer solution was still ≈20%, which implied that ≈80% of the BP-nanodots had been ionized as P_xO_y (e.g., phosphates and phosphonates). For surface passivation characterization in BP-nanodots, analysis of elemental binding of P_{2p} in BP-nanodots was examined by

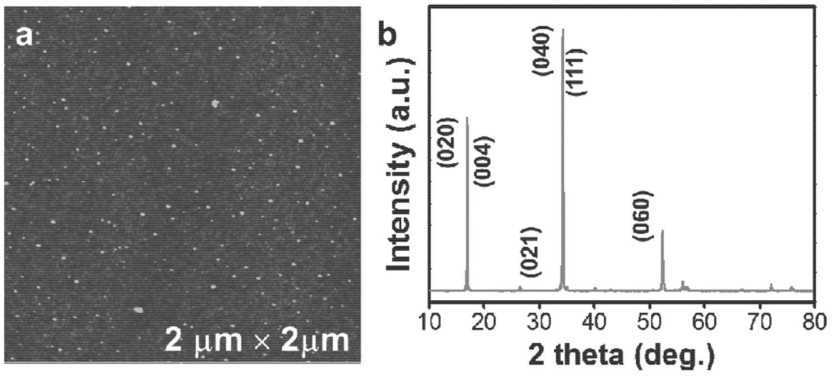

Figure 1. Characterizations of BP-nanodots. a) Representative AFM characterization showing disperse nanoparticle formation of BP-nanodots on SiO2/Si substrate and b) X-ray diffraction (XRD) patterns of BP-nanodots.

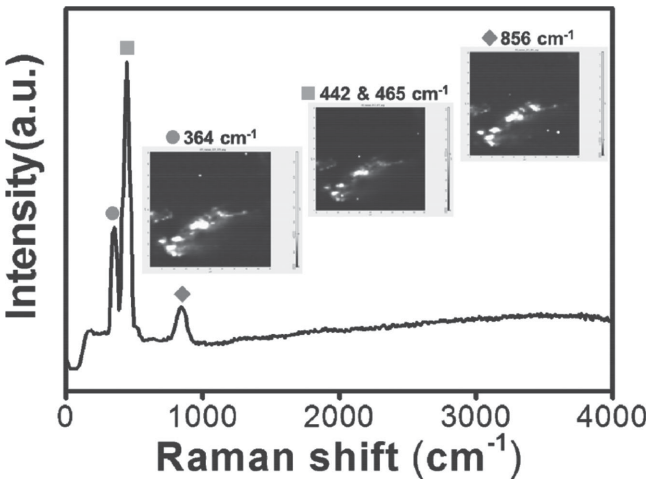

Figure 2. Raman spectrum and mapping images at 364, 442, 465, and 856 cm^{-1} of BP-nanodots.

X-ray photoelectron spectroscopy (XPS) (Supporting Information, Figure S3). It revealed 129.8/130.7 eV at $2P_{3/2}/2P_{1/2}$ of P^{3+} and 133.4 eV at P^{5+}, respectively,[18] which is associated with PL spectra patterns. Also, the internal quantum yield of BP-nanodots was measured to be ≈1.9%. In order to reconfirm the blue, green, and red fluorescence emissions, the 220, 234, 280, and 370 nm excitation wavelengths were investigated (Supporting Information, Figure S4). Significantly, the blue and green fluorescence emissions were strongly detectable but the red was very weak.

For the cell viability and bioimaging of BP-nanodots, preliminarily to prospective biomedical applications, BP-nanodots and ionized BP-nanodots (0–3.0 mg mL^{-1}) at 12 h were assayed (**Figure 4**). The BP-nanodot crystals' cell viabilities showed no or little cytotoxic effects in vitro at 1.0 mg mL^{-1} for HeLa, COS-7, and CHO-K1 cells, but only ≈90% at 3.0 mg mL^{-1} (Figure 4a), due to necrosis cell death by the excess crystalline-structured BP-nanodots. Further ionization of the BP-nanodots at 3.0 mg L^{-1} resulted in no or negligible cytotoxic effects for the HeLa and COS-7 cells also (Figure 4b). For 24 and 48 h incubations with ionized BP-nanodots, it also showed little cytotoxicities upto at 3 mg mL^{-1} (Supporting Information Figure S5). Based on the optical properties of the BP-nanodots as demonstrated in confocal microscopy images of their uptake in HeLa cells (**Figure 5**), it was emitted a blue color in the HeLa cells under UV light excitation (Figure 5a–c) and green under visible light excitation (Figure 5d–f), compared to no fluorescent intensity in HeLa cells without BP-nanodots treatment (Supporting Information, Figure S6). The fluorescent images of the HeLa cells with BP-nanodots are taken under both excitations of UV and visible lights for providing multiple colors. Therefore, BP can be utilized in biomedical applications as blue- and green-emission bioimaging probes.

In the literature, significantly rich and varied, 2D graphene[25] and its analogues such as metal dichalcogenides and transition metal oxides[1,2,10] have emerged as new platforms for bioprobes. The research has focused on in vitro cellular uptake/location/toxicity and in vivo biodistribution/degradation/excretion of inorganic 2D materials. It was found that exfoliated MoS_2 and WS_2 nanosheets offer even lower cytotoxicity than graphene-based materials. The TMDCs showed low cytotoxicity at extremely low concentration (<0.10 mg mL^{-1}), indicating its biomedical potential.[25] However, methods above suffer from removal process by clearance/excretion of TMDCs directly, which limit their wide biomedical applications. For practical use in medicine, BP-nanodots are desirable because BP can be instabilized to ionize as phosphate ion form.

In the present study, over the course of 10 d, ≈20% of the BP-nanodots remained in the crystalline-structural form. In line with the logic of BP-nanodot's instability in aqueous solution, our in vitro animal-cell viability results showed, unprecedentedly, no or little cytotoxicity at 1.0 mg mL^{-1}. In the adult human body, the concentration of phosphorus is known to be ≈0.87–1.45 mmol L^{-1} (i.e., 0.028–0.047 mg L^{-1}), which consists of ≈85% main skeleton or bone and ≈15% soft tissue.[28] Compared with the lesser biodegradation of TMDCs, BP-nanodots could serve as a smart detoxified delivery carrier in biomedical applications, particularly when considering blood-circulation duration. Thus, we are currently utilizing BP-nanodots in systematic internal-stress-based

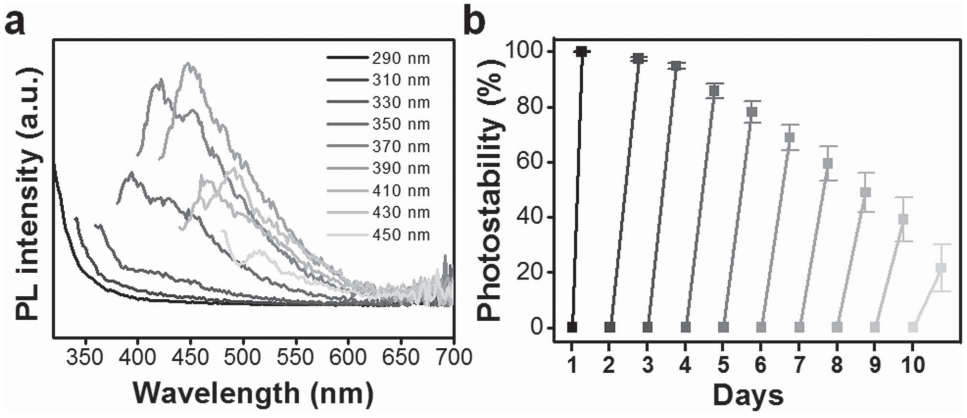

Figure 3. Optical properties of fluorescence BP-nanodots. a) Photoluminescence (PL) spectra of BP-nanodots at different excitation wavelengths within the 290–450 nm range. b) Photostability measurements of suspended BP-nanodots are in the 1–10 d range; all excitation spectra were recorded for respective emission maxima.

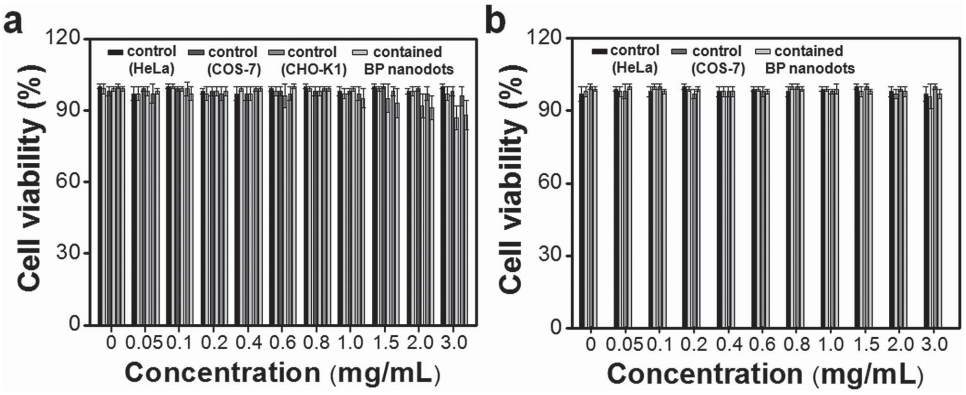

Figure 4. Biocompatability testing of BP-nanodots for 12 h. Cell viability of HeLa, COS-7, and CHO-K1 cells after incubation with BP-nanodots suspension at different a) BP-nanodots and b) ionized BP-nanodot concentrations, showing nontoxicity at concentrations less than 1.0 mg mL^{-1}.

cell-toxicity and anticancer therapeutics for in vivo tumor-bearing mice.

In summary, we fabricated a new class of fluorescent BP-nanodots from BP using an exfoliated solution method with modified ultrasonication. The BP-nanodots were demonstrated to be stable for 10 d in aqueous solution and to exhibit excitation wavelength-dependent PL characteristics, thereby emitting multiple colors (blue and green). It is discovered that BP-nanodots can be utilized in HeLa cell imaging with a good PL signal and low cytotoxicity. Compared other nanodots, BP nanodots possess biocompatibility and expect spontaneous degradability in bodily systems with no or little cytotoxicity, simultaneously having fluorescent emission for potential bioprobe applications. Most importantly, this study indicates that these BP-nanodots have great potential for biomedical applications including bioimaging, drug delivery, and cellular tracking.

3. Experimental Section

Preparation of BP-Nanodots: In the typical synthesis,[18] black phosphorous (BP, 0.4 g, 12.8 mmol) was dispersed in distilled (DI) water (100 mL) by high-intensity ultrasound irradiation for 30 min, thereby forming several-layered BP-nanodots. The sample was maintained at room temperature for 10 min. 10 mL supernatant liquid was collected from the dispersion solution, dissolved in DI water (100 mL), and ultrasound-irradiated for 10 min. These steps were repeated two more times to afford BP particles. Dispersion of the BP-nanodots was performed under high-intensity ultrasound of 20 kHz frequency applied from the top of a polypropylene bottle reactor (≈40 mL) using a Sonics and Materials VC750 ultrasonic generator and maintaining 100 W electrical energy input.

Characterization: The UV–vis absorbance spectra of the BP-nanodots at 1.0, 0.5, and 0.25 mg L^{-1} concentrations were recorded by UV–vis spectrophotometry (Varian, Cary 50 Bio). PL

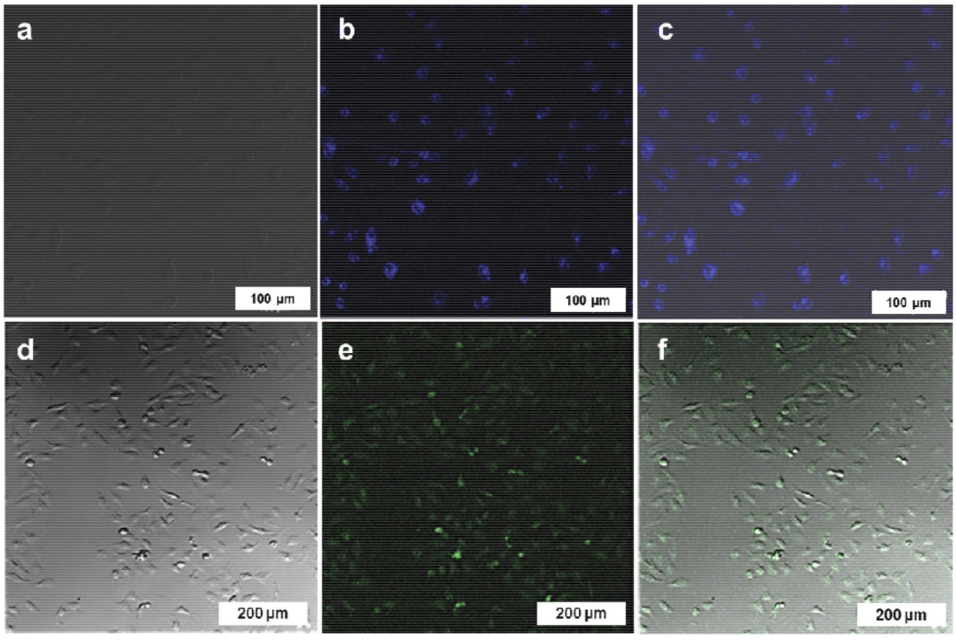

Figure 5. Cell bioimaging of BP-nanodots. Confocal microscopy images of live HeLa cells after 12 h incubation with 1 mg mL^{-1} BP-nanodots suspension. a,d) bright field (BF) and b,e) fluorescence (FL), and merged c,f) images. Detection of BP-nanodots fluorescence was achieved by excitation at (b) 358 nm and (e) 488 nm, with a 30 mW Argon laser.

emissions of the BP-nanodots at the 1.0 mg mL^{-1} concentration with excitation wavelengths of 290, 310, 330, 350, 370, 390, 410, 430, and 450 nm were measured using a multimicroplate reader (Synerg H1, Bioteck). The crystalline structure of the BP-nanodots was investigated with reference to the X-ray diffraction (XRD; Rigaku RDA-cA X-ray diffractometer, Japan) patterns obtained by passing Cu Kα radiation through a nickel filter. The morphology of the BP-nanodots was observed by high-resolution transmission electron microscopy (HR-TEM; JEOL, JEM 2200, Japan). The morphological structure and size of the BP-nanodots were analyzed by atomic force microscopy (AFM, Digital Instruments, Santa Barbara, USA). For the AFM analysis, 100 µL of the BP-nanodots solution was placed on a SiO_2/Si wafer. The wafer was air-dried for 24 h, and the remaining solution was dispersed using an air gun. An He-Cd laser (Kimmon, 1K, Japan) of 325 nm wavelength and 50 mW power was employed as an excitation source for PL measurements carried out using a spectrograph (f = 0.5 m, Acton Research Co., Spectrograph 500i, USA) with an intensified charge-coupled device (CCD, PI-MAX3, Princeton Instruments, IRY1024, USA). According to literature,[29] the internal quantum yield was measured with the Quantum Yield System (K-MAC, Fluoro-Q2100) at 370 nm excitation on the basis of equation: Quantum yield = Ec/(La–Lc), where Ec is the emission produced by direct excitation light, La is the total amount of excitation light, and Lc is the amount of light after direct excitation. Raman spectroscopy also was performed (Renishaw, RM1000-Invia) in a backscattering configuration excited with a visible laser light (wavelength = 514 nm), a notch filter cut-off frequency of 50 cm^{-1}, and a focus spot size of 5 µm. Spectra were collected through a 100× objective lens and recorded on a 1800 lines mm^{-1} grating providing a spectral resolution of ≈1 cm^{-1}. To avoid laser-induced heating and ablation of the samples, all of the spectra were recorded at low power levels (≈0.1 mW) and short integration times (≈5 s). The internal quantum yield (3 mg mL^{-1} of BP-nanodots) of BP-nanodots was measured by spectrofluorometer (FP-8500, Jasco, Japan): excitation wavelength 370 nm; emission wavelength 380–700 nm; response 0.1 s; PMT voltage 300; scan speed 1000 nm min^{-1}; data interval 0.1 nm; bandwidth 5 nm.

Cytotoxicity Assays and Bioimaging of BP-Nanodots: The cytotoxicities of the BP-nanodots were evaluated by 3-(4,5-dimethylthiazol-2-yl)-2,5-diphenyltetrazolium bromide (MTT) assay. Briefly, CHO-K1, COS-7, and HeLa cells were seeded in a 96-well plate at a density of 9×10^3 cells per well and cultured in a humidified incubator at 37 °C for 24 h under a 5% CO_2 atmosphere in Dulbecco's modified Eagle's medium (DMEM) or Roswell Park Memorial Institute (RPMI)-1640 supplemented with 10% FBS and 1% penicillin-streptomycin antibiotics in DI water and/or ionized BP-nanodots solution. Then, 20 µL of a 0.2 mg mL^{-1} MTT solution in DMEM and/or RPMI-1640 was added to each well and incubated at 37 °C for 2 h. Finally, the optical density was measured at 490 nm with an absorbance microplate reader (EMax microplate reader, Bucher Biotec AG, Basel, Switzerland). HeLa cells were cultured on an 6-well plate at a concentration of 2×10^5 cells per well for confocal microscope (LSM510 META NLO, Carl Zeiss, Germany) at blue and green fluorescence with excitation at 358 nm/emission at 461 nm and excitation at 488 nm/emission at 509 nm, respectively.

Statistical Analysis: All of the data were averaged and expressed as mean ± standard error deviations (SE). Each test was repeated up to five times. Analysis of variance (ANOVA) as a statistical model was performed, wherein p-values less than 0.05 were considered significant.

Supporting Information

Supporting Information is available from the Wiley Online Library or from the author.

Acknowledgements

H.U.L. and S.Y.P. contributed equally to this work. This research was supported by KBSI research under Grant No. E35800.

[1] S. Balendhran, S. Walia, H. Nili, S. Sriram, M. Bhaskaran, *Small* **2015**, *11*, 640.
[2] H. O. H. Churchill, P. Jarillo-Herrero, *Nat. Nanotechnol.* **2014**, *9*, 330.
[3] L. Li, Y. Yu, G. J. Ye, Q. Ge, X. Ou, H. Wu, D. Feng, X. H. Chen, Y. Zhang, *Nat. Nanotechnol.* **2014**, *9*, 372.
[4] F. Xia, H. Wang, Y. Jia, *Nat. Commun.* **2014**, *5*, 4458.
[5] J. Qiao, X. Kong, Z.-X. Hu, F. Yang, W. Ji, *Nat. Commun.* **2014**, *5*, 4475.
[6] L. Wang, X. He, J. Li, W. Sun, J. Gao, J. Guo, C. Jiang, *Angew. Chem., Int. Ed.* **2012**, *51*, 9034.
[7] M. Buscema, D. J. Groenendijk, G. A. Steele, H. S. J. van der Zant, A. Castellanos-Gomez, *Nat. Commun.* **2014**, *5*, 4651.
[8] D. Hanlon, C. Backes, E. Doherty, C. S. Cucinotta, N. C. Berner, C. Boland, K. Lee, P. Lynch, Z. Gholamvand, A. Harvey, S. Zhang, K. Wang, G. Moynihan, A. Pokle, Q. M. Ramasse, N. McEvoy, W. J. Blau, J. Wang, S. Sanvito, D. D. O'Regan, G. S. Duesberg, V. Nicolosi, J. N. Coleman,*Nat. Commun.*, **2015**, *6*, 8563.
[9] H. Liu, Y. Du, Y. Deng, P. D. Ye, *Chem. Soc. Rev.* **2015**, *44*, 2732.
[10] X. Ling, H. Wang, S. Huang, F. Xia, M. S. Dresselhaus, *Proc. Natl. Acad. Sci. USA* **2015**, *112*, 4523.
[11] Y. Du, H. Liu, Y. Deng, P. D. Ye, *ACS Nano* **2014**, *8*, 10035.
[12] J. Na, Y. T. Lee, J. A. Lim, D. K. Hwang, G.-T. Kim, W. K. Choi, Y.-W. Song, *ACS Nano* **2014**, *8*, 11753.
[13] J. D. Wood, S. A. Wells, D. Jariwala, K.-S. Chen, E. K. Cho, V. K. Sangwan, X. Liu, L. J. Lauhon, T. J. Marks, M. C. Hersam, *Nano Lett.* **2014**, *14*, 6964.
[14] J. Dai, X. C. Zeng, *RSC Adv.* **2014**, *4*, 48017.
[15] A. Favron, E. Gaufrès, F. Fossard, A.-L. Phaneuf-L'Heureux, N. Y.-W. Tang, P. L. Lévesque, A. Loiseau, R. Leonelli, S. Francoeur, R. Martel, *Nat. Mater.* **2015**, *14*, 826.
[16] H. Zhu, X. Qin, A. Azcatl, R. Addou, S. McDonnell, P. D. Ye, R. M. Wallace, *Microelectron. Eng.* **2015**, *147*, 1.
[17] P. Mal, B. Breiner, K. Rissanen, J. R. Nitschke, *Science* **2009**, *324*, 1696.
[18] H. U. Lee, S. C. Lee, J. Won, B.-C. Son, S. Choi, Y. Kim, S. Y. Park, H.-S. Kim, Y.-C. Lee, J. Lee, *Sci. Rep.* **2015**, *5*, 8691.
[19] M. Engel, M. Steiner, P. Avouris, *Nano Lett.* **2014**, *14*, 6414.
[20] J. Dai, X. C. Zeng, *J. Phys. Chem. Lett.* **2014**, *5*, 1289.
[21] L.-Q. Sun, M.-J. Li, K. Sun, S.-H. Yu, R.-S. Wang, H.-M. Xie, *J. Phys. Chem. C* **2012**, *116*, 14772.
[22] J. Sun, G. Zheng, H.-W. Lee, N. Liu, H. Wang, H. Yao, W. Yang, Y. Cui, *Nano Lett.* **2014**, *14*, 4573.
[23] Y. Yang, A. M. Asiri, Z. Tang, D. Du, Y. Lin, *Mater. Today* **2013**, *16*, 365.

[24] H. Shen, L. Zhang, M. Liu, Z. Zhang, *Theranostics* **2012**, *2*, 283.
[25] Y. Chen, C. Tan, H. Zhang, L. Wang, *Chem. Soc. Rev.* **2015**, *44*, 2681.
[26] X. Zhang, H. Xie, Z. Liu, C. Tan, Z. Luo, H. Li, J. Lin, L. Sun, W. Chen, Z. Xu, L. Xie, W. Huang, H. Zhang, *Angew. Chem., Int. Ed.* **2015**, *54*, 3653.
[27] P. Yasaei, B. Kumar, T. Foroozan, C. Wang, M. Asadi, D. Tuschel, J. E. Indacochea, R. F. Klie, A. Salehi-Khojin, *Adv. Mater.* **2015**, *27*, 1887.
[28] Phosphate in Blood, http://www.webmd.com/a-to-z-guides/phosphate-in-blood?page=3 (accessed: June 2015)
[29] S. Y. Park, H. U. Lee, Y.-C. Lee, S. Choi, D. H. Cho, H. S. Kim, S. Bang, S. Seo, S. C. Lee, J. Won, B.-C. Son, M. Yang, J. Lee, *Sci. Rep.* **2015**, *5*, 12420.

Received: September 10, 2015
Revised: October 5, 2015
Published online: November 20, 2015